[PROC. OF JSCE No. 369/II-5 (Hydraulic and Sanitary Eng.) May 1986/Technical Note]

A CONFORMAL MAPPING OF A FINITE REGION BOUNDED BY WAVY WALLS

*By Hitoshi Tanaka**

A conformal mapping of a finite region bounded by wavy boundaries is proposed. A modification leads to a transform function of the semi-infinite region over an asymmetric rippled bed. The technique can be extensively applied to the analysis of the two-dimensional fluid motion bounded by wavy boundaries.

1. INTRODUCTION

Fluid motion over a wavy wall has been studied by many researchers in connection with problems of such as wave generation by wind and sediment movement over a rippled bed. For an analysis of the fluid motion bounded by a wavy surface, it is convenient to work on transformed curvilinear coordinates. Conformal mappings defined by Eqs. (1) or (2) are often used in analytical and numerical investigations (e.g. refs. 1), 2), 3)).

$$\zeta = z - i\frac{\eta}{2}e^{ikz} \quad \cdots\cdots (1)$$

$$z = \zeta + i\frac{\eta}{2}e^{ik\zeta} \quad \cdots\cdots (2)$$

where

$$\zeta = \alpha + i\beta \quad \cdots\cdots (3)$$

$$z = x + iy \quad \cdots\cdots (4)$$

k is the wave number ($k=2\pi/\lambda$, λ : wavelength), and η is the parameter associated with the wave height of the wavy boundary. In case of Eq. (2), η exactly gives the crest-to-trough height.

Equations (1) or (2) give the relation between the orthogonal curvilinear coordinates (α, β) and the Cartesian coordinates (x, y) as shown in Fig. 1.

The wavy surface given by Eq. (2) has pointed crests and flatter troughs. Therefore, the shape of sand ripples generated by the

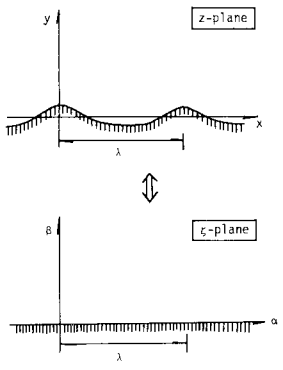

Fig. 1 Transformation defined by Eqs. (1) or (2).

* Member of JSCE Dr. Eng., Research Associate, Dept. of Civil Eng., Utsunomiya University (Ishii, Utsunomiya, 321)

purely oscillatory motion is well approximated by Eq. (2), rather than by Eq. (1). It should be noted, however, that surface profiles given by Eqs. (1) or (2) are symmetric with respect to the crest.

Under many practically important hydraulic conditions, sand ripples are no longer symmetric with respect to the crest. Waves in shallow sea make sand ripples asymmetric. This is considered as an effect of nonlinearity. If a steady flow such as nearshore currents or river flow is added to waves, the asymmetry of sand ripples may be more and more developed. Therefore, applicability of Eqs. (1) and (2) is rather restricted and another transform function such as that used by Sato et al.[4] is required.

In the present paper, a transform function is proposed on the basis of Eq. (2), in order to map a finite region bounded by two asymmetric wavy boundaries at the upper and lower ends onto a rectangle. A modification leads to a conformal mapping of the semi-infinite region over an asymmetric rippled bed onto the upper half plane. Other applications of the present technique may also be found in the analysis of river flow such as flow in meandering channels and streamlines over dunes or antidunes.

2. TRANSFORM FUNCTION

When the wave height to wavelength ratio, η/λ, is considerably small, Eq. (2) gives sinusoidal boundary profile as is seen in Eq. (5).

$$x=\alpha \quad \cdots\cdots (5\cdot a)$$

$$y=\frac{\eta}{2}\cos k\alpha \quad \cdots\cdots (5\cdot b)$$

Therefore, when we consider the finite region such as that shown in Fig. 2, Eq. (6) is available on the analogy of a Fourier series. It should be noted that the wavy walls are assumed to be periodical in the x-direction with the wavelength λ.

$$z=\zeta+i\left[\sum_{j=1}^{n} a_j e^{ijk(\alpha+i\beta-i\beta_1)+\theta_j i}+\sum_{j=1}^{n} b_j e^{-ijk(\alpha+i\beta-i\beta_2)+\phi_j i}\right] \quad \cdots\cdots (6)$$

Equating real and imaginary parts of Eq. (6), we have Eq. (7), which is presented in dimensionless form convenient for practical application.

$$x^*=\alpha^*-S_1\sum_{j=1}^{n} a_j^* e^{-2\pi j(\beta^*-\beta_1^*)}\sin(2\pi j\alpha^*+\theta_j)+S_2\sum_{j=1}^{n} b_j^* e^{2\pi j(\beta^*-\beta_2^*)}\sin(2\pi j\alpha^*+\phi_j) \quad \cdots\cdots (7\cdot a)$$

$$y^*=\beta^*+S_1\sum_{j=1}^{n} a_j^* e^{-2\pi j(\beta^*-\beta_1^*)}\cos(2\pi j\alpha^*+\theta_j)+S_2\sum_{j=1}^{n} b_j^* e^{2\pi j(\beta^*-\beta_2^*)}\cos(2\pi j\alpha^*+\phi_j) \quad \cdots\cdots (7\cdot b)$$

The superscript * in the above equations denotes the non-dimensional quantities defined as follows.

$x^*=x/\lambda$, $y^*=y/\lambda$, $\alpha^*=\alpha/\lambda$, $\beta^*=\beta/\lambda$, $a_j^*=a_j/\eta_1$, $b_j^*=b_j/\eta_2$, $S_1=\eta_1/\lambda$, $S_2=\eta_2/\lambda$, $\beta_1^*=\beta_1/\lambda$, $\beta_2^*=\beta_2/\lambda$

where, η_1 and η_2 denote the crest-to-trough height of the lower and upper boundaries, respectively.

By Eq. (7), two horizontal lines given by $\beta=\beta_1$ and $\beta=\beta_2$ in the ζ-plane are transformed to the lower and upper wavy boundaries in the z-plane as seen in Fig. 2.

Lower boundary is given by

$$x^*=\alpha^*+\sum_{j=1}^{n}(C_j^{(1)}\sin 2\pi j\alpha^*+C_j^{(2)}\cos 2\pi j\alpha^*) \quad \cdots\cdots (8\cdot a)$$

$$y^*=\beta_1^*+\sum_{j=1}^{n}(D_j^{(1)}\cos 2\pi j\alpha^*-D_j^{(2)}\sin 2\pi j\alpha^*) \quad \cdots\cdots (8\cdot b)$$

Upper boundary is given by

$$x^*=\alpha^*+\sum_{j=1}^{n}(E_j^{(1)}\sin 2\pi j\alpha^*+E_j^{(2)}\cos 2\pi j\alpha^*) \quad \cdots\cdots (9\cdot a)$$

$$y^*=\beta_2^*+\sum_{j=1}^{n}(F_j^{(1)}\cos 2\pi j\alpha^*-F_j^{(2)}\sin 2\pi j\alpha^*) \quad \cdots\cdots (9\cdot b)$$

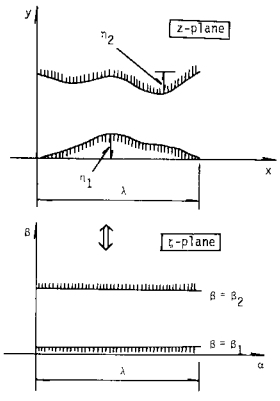

Fig. 2 Transformation of a finite region.

where

$$C_j^{(1)}=-S_1a_j^*\cos\theta_j+S_2b_j^*e^{2\pi j(\beta_1^*-\beta_2^*)}\cos\phi_j \quad (10\cdot a)$$

$$C_j^{(2)}=-S_1a_j^*\sin\theta_j+S_2b_j^*e^{2\pi j(\beta_1^*-\beta_2^*)}\sin\phi_j \quad (10\cdot b)$$

$$D_j^{(1)}=S_1a_j^*\cos\theta_j+S_2b_j^*e^{2\pi j(\beta_1^*-\beta_2^*)}\cos\phi_j \quad (10\cdot c)$$

$$D_j^{(2)}=S_1a_j^*\sin\theta_j+S_2b_j^*e^{2\pi j(\beta_1^*-\beta_2^*)}\sin\phi_j \quad (10\cdot d)$$

$$E_j^{(1)}=-S_1a_j^*e^{-2\pi j(\beta_2^*-\beta_1^*)}\cos\theta_j+S_2b_j^*\cos\phi_j \quad (10\cdot e)$$

$$E_j^{(2)}=-S_1a_j^*e^{-2\pi j(\beta_2^*-\beta_1^*)}\sin\theta_j+S_2b_j^*\sin\phi_j \quad (10\cdot f)$$

$$F_j^{(1)}=S_1a_j^*e^{-2\pi j(\beta_2^*-\beta_1^*)}\cos\theta_j+S_2b_j^*\cos\phi_j \quad (10\cdot g)$$

$$F_j^{(2)}=S_1a_j^*e^{-2\pi j(\beta_2^*-\beta_1^*)}\sin\theta_j+S_2b_j^*\sin\phi_j \quad (10\cdot h)$$

In order to determine the unknown coefficients a_j^*, b_j^*, θ_j, ϕ_j, β_1^* and β_2^* in Eqs. (8) and (9), the following procedure is employed.

(1) Determine the coordinates y_m^* for equally spaced values of $x_m^*(m=1,2,\cdots,l)$ on both the wavy boundaries, for which we are going to apply the conformal transformation.

(2) Perform harmonic analysis for both boundaries using the data $y_m^*(m=1,2,\cdots,l)$ obtained in (1).

(3) Let the results of the harmonic analysis be the first approximations of a_j^*, b_j^*, θ_j, ϕ_j, β_1^* and β_2^*.

(4) Solve Eqs. (8·a) and (9·a) with respect to $a_m^*(m=1,2,\cdots,l)$ by the Newton-Raphson method.

(5) Substitute $a_m^*(m=1,2,\cdots,l)$ into Eqs. (8·b) and (9·b). Then, solve them with respect to β_1^*, $D_j^{(1)}$, $D_j^{(2)}$, β_2^*, $F_j^{(1)}$ and $F_j^{(2)}$ by the multiple linear regression analysis. The second approximation of the solution can be obtained by the following expressions, taking account of Eqs. (10·c), (10·d), (10·g) and (10·h).

$$a_j^*=[|\gamma_j^{(1)}|^2+|\gamma_j^{(2)}|^2]^{1/2} \quad (11\cdot a)$$

$$\theta_j=\tan^{-1}(\gamma_j^{(2)}/\gamma_j^{(1)}) \quad (11\cdot b)$$

$$b_j^*=[|\delta_j^{(1)}|^2+|\delta_j^{(2)}|^2]^{1/2} \quad (12\cdot a)$$

$$\phi_j=\tan^{-1}(\delta_j^{(2)}/\delta_j^{(1)}) \quad (12\cdot b)$$

where

$$\gamma_j^{(1)}=a_j^*\cos\theta_j=\frac{D_j^{(1)}e^{2\pi j(\beta_2^*-\beta_1^*)}-F_j^{(1)}}{2S_1\sinh 2\pi j(\beta_2^*-\beta_1^*)} \quad (13\cdot a)$$

$$\gamma_j^{(2)}=a_j^*\sin\theta_j=\frac{D_j^{(2)}e^{2\pi j(\beta_2^*-\beta_1^*)}-F_j^{(2)}}{2S_1\sinh 2\pi j(\beta_2^*-\beta_1^*)} \quad (13\cdot b)$$

$$\delta_j^{(1)}=b_j^*\cos\phi_j=-\frac{D_j^{(1)}-F_j^{(1)}e^{2\pi j(\beta_2^*-\beta_1^*)}}{2S_2\sinh 2\pi j(\beta_2^*-\beta_1^*)} \quad (13\cdot c)$$

$$\delta_j^{(2)}=b_j^*\sin\phi_j=-\frac{D_j^{(2)}-F_j^{(2)}e^{2\pi j(\beta_2^*-\beta_1^*)}}{2S_2\sinh 2\pi j(\beta_2^*-\beta_1^*)} \quad (13\cdot d)$$

(6) If the difference between the first and second approximations is not sufficiently small, return to the step (4) after replacing the first approximations with the refined values. Repeat the above calculation until the difference becomes small enough.

3. EXAMPLES OF THE TRANSFORMATION

The first example of the technique is computed for a geometry shown in Fig. 3. The lower wave is almost symmetric with the height-to-length ratio 0.145 while the upper wave of the height-to-length ratio 0.160 is asymmetric and has its crest at $x^*=0.68$. It is, of course, assumed that this geometry repeats with the length $x^*=1$ in the x^*-direction.

In Figs. 4, 5 and 6, accuracy of the transform which depends on the number of terms included in the series is

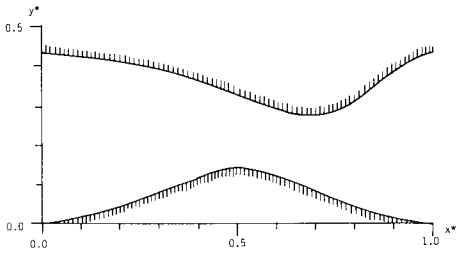

Fig. 3 Finite region bounded by wavy walls.

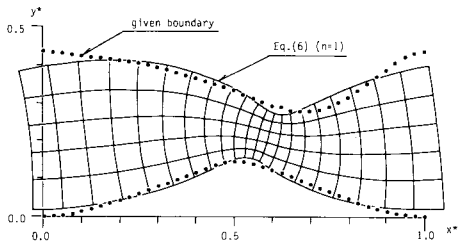

Fig. 4 Flow net in the z-plane given by Eq. (6) (n=1).

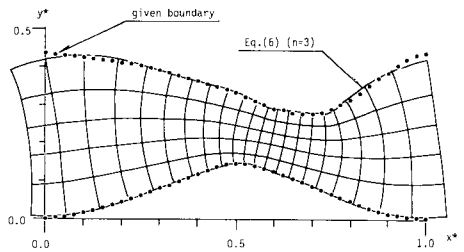

Fig. 5 Flow net in the z-plane given by Eq. (6) (n=3).

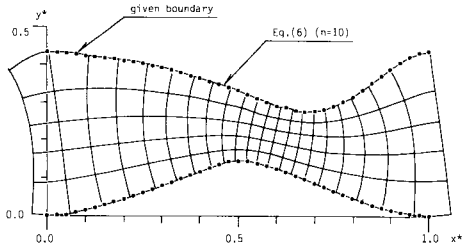

Fig. 6 Flow net in the z-plane given by Eq. (6) (n=10).

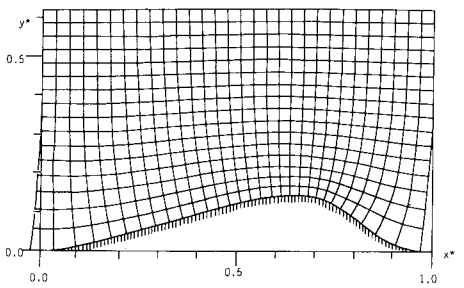

Fig. 7 Flow net over an asymmetric wavy boundary.

shown. Dotted lines are the given profiles of the upper and lower boundaries. Computed streamlines and equi-potential lines are shown by full lines. Examination of the accuracy is carried out by comparing the shape of upper and lower streamlines with the given boundaries.

With n=1 which tells that only the first term in the series is included in the computation, agreement is not satisfactory, especially for the upper boundary. The position of the computed crest appears at smaller x^* than that of the assumed crest. Agreement is better for the lower boundary. Many terms are neccessary to express an asymmetric profile. With n=3, the agreement is improved but the shape of the computed upper streamline is not smooth. If the number of terms increases up to ten, the result becomes satisfactory.

The second example is to obtain a flow net over an asymmetric ripple without the upper boundary. If we let $b_j^*=0$ and $\beta_2^*\to\infty$, this condition is satisfied. The model ripple in the example has the height-to-length ratio of 0.142. Its crest is at $x^*=0.69$. The result for n=10 is shown in Fig. 7.

4. CONCLUSION

A conformal mapping of a finite region bounded by wavy boundaries is proposed. The technique can be extensively applied to the analysis of the two-dimensional fluid motion bouned by wavy boundaries.

ACKNOWLEDGEMENT

The author would like to express his thanks to Professor N. Shuto, Tohoku University, and Professor K. Suga, Utsunomiya University, for their helpful advice over the course of this study.

REFERENCES

1) Benjamin, T. B. : Shearing flow over a wavy boundary, Jour. Fluid Mech., Vol. 6, pp. 161~205, 1959.
2) Du Toit, C. G. and Sleath J. F. A : Velocity measurements close to rippled beds in an oscillatory flow, Jour. Fluid Mech. Vol. 112, pp. 71~96, 1981.
3) Sawamoto, M. : The conformal mapping of the semi-infinite region over a wavy boundary, Proc. J. S. C. E., No. 269, pp. 147~150, 1978 (in Japanese).
4) Sato, S., Mimura N. and Watanabe A. : Oscillatory boundary layer flow above rippled bed, Proc. 30 th Japanese Conf. Coastal Engng., pp. 189~193, 1983 (in Japanese).

(Received June 22 1985)